Inductive Coupling and Flow for Increased NMR Sensitivity

Guillaume Carret, Thomas Berthelot, Patrick Berthault

Inductive Coupling and Flow for Increased NMR Sensitivity

Guillaume Carret, Thomas Berthelot, and Patrick Berthault*

NIMBE, CEA, CNRS, Paris-Saclay University, CEA Saclay, 91191 Gif-sur-Yvette, France

KEYWORDS: NMR ; relaxation ; sensitivity ; 3D printing ; micro-detection

ABSTRACT: A device is proposed to enhance the NMR sensitivity of slowly-relaxing nuclei, taking advantage of a controlled solution flow within a microfluidic circuit and micro-sized NMR detection. At the difference of our previous work (Carret at al., *Anal. Chem.* **2017**, *89* (5), 2995–3000), this set-up can be easily installed on any commercial NMR probehead as it uses induction between the commercial antenna and the micro-coil. Such a system leads to a significant gain in sensitivity per time unit for slowly relaxing nuclei while preserving the capabilities of the host probehead.

NMR is a versatile but very insensitive technique, especially for slowly-relaxing nuclei. In liquid-state NMR, the hardware solutions proposed so far to overcome the problems inherent in the slow return of magnetization to equilibrium range from a recycled solution flow[1] to the use of immobilized paramagnetic species.[2] Recently we presented a 3D-printed NMR device based on a mini bubble-pump associated to fluidics and micro-detection that can be installed on a commercial micro-imaging NMR probe head.[3] In addition to properties such as enabling efficient enrichment of the solution in gaseous hyperpolarized species or in gaseous nutriments for cells, it leads to a significant signal enhancement for slowly relaxing nuclei.[4] As between two scans fresh spins replace previously excited ones in the detection region, there is no need to wait for several relaxation times. Our approach based on the use of a closed-loop circuit at the NMR magnetic center for the solution presents two main advantages in addition to its low cost: i) pre-polarization is achieved for the whole solution volume, ii) this volume can be reduced to some tens of microliters.

However, this setup implied plugging the 3D-printed NMR insert onto a micro-imaging NMR probe head body. This limits the versatility of the method, since the mini flow-NMR device is associated to a specific commercial probe.

To address this issue, we had to conceive a new device, which could fit in liquid-state NMR probeheads. Since we are working with a microfluidic circuit, we cannot rely solely on the coil of the commercial probehead to detect the NMR signal, since we would have a poor filling factor, compared to a cylindrical NMR tube adjusted to the diameter of the probehead.[5] Indeed, a single loop of solution flowing into a tube of 1 mm diameter inside a 10 mm probe would have a hundred times lower filling factor compared to an NMR tube, which would reduce the signal-to-noise ratio (SNR) by a factor of ten, thereby opposing the signal enhancement due to the solution flow.[4]

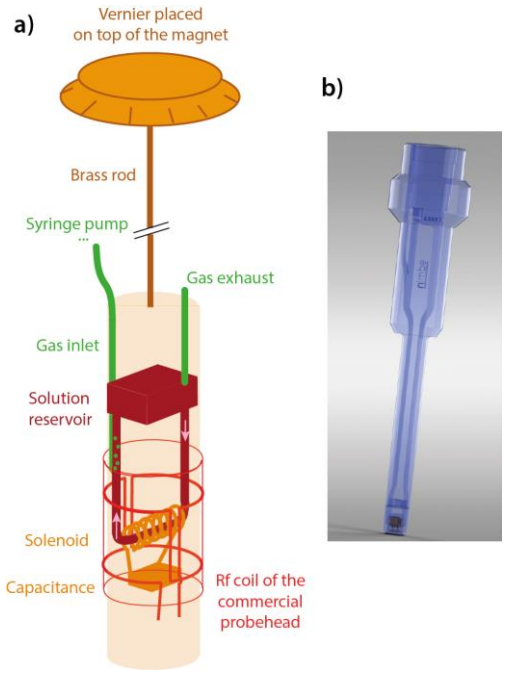

Figure 1. a) Schematic drawing of the *WIFI-NMRS* device. The red parts correspond to the commercial probehead on which it is installed. b) 3D-rendering of the NMR insert.

In order to improve the coupling between the pickup coil and the sample without modifying the commercial probehead, an inductively-coupled scheme can be used, where a resonator is used to shape the rf magnetic field lines, strengthening the irradiation field in the region of interest and, due to the reciprocity theorem,[6] increasing the sensitivity in this region. This solution is a very popular way to wirelessly transmit data or even energy with a high power efficiency,[7] and has widely been used in MRI[8–12] and in solid-state NMR spectroscopy for the MACS ('Magic Angle Coil Spinning') approach.[13] The methods for calculating and improving the inductive coupling between two coils are also well documented.[14–17]

The idea here is to introduce the assembly containing the 3D-printed microfluidics, the NMR coil and the capacitance through the top of the NMR magnet, as would be the case for any liquid sample (Figure 1a). Outside the spectrometer the reservoir and the fluidic channels drawn in dark red in Fig. 1a are filled with the solution by using a normal micropipette, and are checked for stuck bubbles. Then a cap attached to a brass rod ended by a Vernier is plugged on the top of the NMR insert. The ensemble is introduced into the magnet bore. The Vernier leans on the top of the magnet, the length of the rod ensuring its perfect vertical positioning with respect to the commercial probehead. Angular positioning of the micro-coil is achieved by manually turning the Vernier.

The solution flow inside the circuit is actuated via a programmable syringe pump that pushes the carrier gas and sets the liquid in motion (see video in Supporting Information S1).[3] Therefore a gas pipe (in green on Fig. 1a) connects the solution circuit in its vertical part to the syringe. This pipe sits in a dedicated channel, visible on the top left of Fig. 1b, which allows for a reliable positioning of the nozzle.

Except for the microcoil, the NMR insert, represented in Fig. 1b, is fully printed via a Polyjet printer (see Supp. Info.). A PMMA-like resin has been chosen for its magnetic susceptibility close to that of water and also because it is transparent. Two pieces are printed: the upper part of the insert contains the reservoir and the fluidic channels; the lower part enables installation of the NMR resonator and closes the solution circuit. Most of the time the detection zone consists of a solenoid wound on a quartz tube. This element is mounted in a carefully designed groove on the 3D printed part, which ensures proper centering of the coil and capillary for each insert. The two pieces are then glued; the detection region is then sealed to improve the homogeneity of the magnetic field. The coil is finally tuned to the frequency of interest.

This device has been dubbed *WIFI-NMRS*, for 'Wireless Inductive coupling & Flow for Increased NMR Sensitivity'. Figure 1b gives a 3D-rendering of the NMR insert. It has the shape of an NMR tube with its spinner, in order to be easily positioned inside the probehead. Only the diameter of the lower part varies to be adjusted to the commercial probehead (from 5 to 20 mm).

Optimization of the coupling between the two coils is made by manually adjusting the angular position of the insert thanks to the Vernier. When this device is inserted in a commercial probe, two resonance dips appear on the wobble curve: one below and one above the original resonance frequency of the probehead, with the splitting between these dips being related to the angle θ between the two coils, as defined in Figure 2a. Using the probe capacitors enables one to match and tune either of these two. This allows one to reach a wide range of frequencies using a single-resonance commercial probehead.

The first series of tests were conducted to characterize the behavior of such an inductively-coupled system, independently from the fluidic circuit. In order to test the NMR signal intensity as a function of the angle θ, in a first step NMR experiments have been performed with the *WIFI-NMRS* system installed on a 10-mm dual broadband/^{1}H probehead. The use of a fast-relaxing nucleus such as ^{23}Na allowed us to study various angular configurations in a reasonable time window. Figure 2b displays the intensity of the ^{23}Na NMR signal, recorded on a saturated solution of NaCl, as a function of the angle θ.

The data were then fitted using a simple cosine function, but it can be observed that the experimental curve is wider at its maxima than at its minima. This behavior is explained by the magnetic field distribution due to this finite-size solenoid (see Fig. S2 of the Supp. Info.).

It can be seen that according to the angle θ a quasi-complete extinction of the signal can be obtained. Precisely, when θ equals 90° the obtained signal is only 4% of the maximum signal. This signal modulation has further been confirmed in ^{23}Na MRI experiments with an 8-mm *WIFI-NMRS* insert placed into a micro-imaging probehead, see Fig. S4 of the Supp. Info.

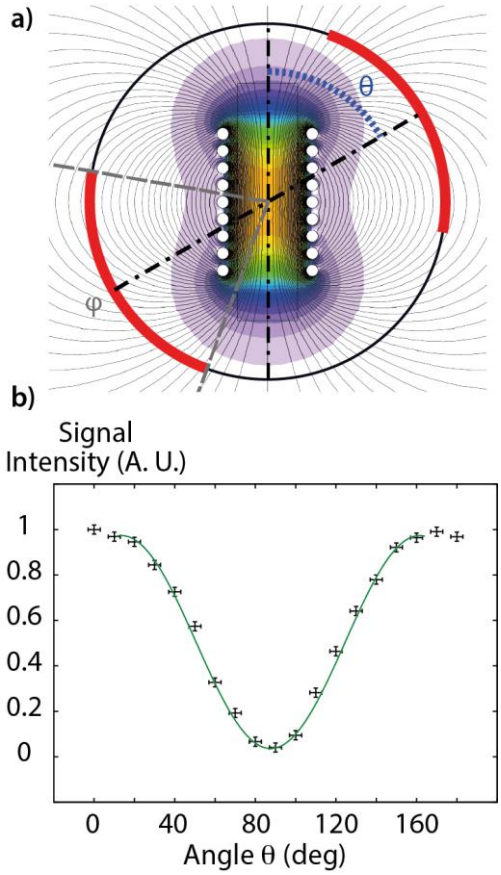

Figure 2. Principle of the *WIFI-NMRS* device. a) View along the static magnetic field axis showing the angle θ between the two radiofrequency fields in interaction. The red lines correspond to the area inside the two loops of the saddle coil. The angle covered by these loops is named φ. The magnetic field represented here ranges from 10^{-4} T (purple) to 1.8 10^{-3} T (orange) for an excitation current of 1 Ampere. b) Intensity of the recorded ^{23}Na NMR signal as a function of the angle θ between the micro-coil axis and the commercial saddle coil of a dual broadband/^{1}H probe. The NMR probe was matched and tuned after each change in angular position.

On these images taken with two different angular positions of the solenoidal coil with respect to the commercial saddle coil, it can be seen that when the two coils are misaligned (θ = 100°) a lower signal intensity is observed. Particularly looking at the radial images, it can be remarked that the extremities of the capillary are brighter than the central part, corresponding to the region of the microcoil. This is the contrary when θ = 0°, emphasizing the effect of the inductive coupling between the two coils.

As previously stated, when the *WIFI-NMRS* device is inserted, two dips appear on the wobble curve. This is due to the fact that the resulting circuit (which is made of two resonant circuits: the *WIFI-NMRS* device and the commercial probe) possesses two poles. By soundly choosing the resonance frequency of the micro-resonator and that of the unloaded commercial probe (with the tuning knobs on a broadband probe) both at the median value of the resonance frequencies of two nuclei separated by less than the difference created by the radiofrequency coupling, a doubly-tuned coil is obtained. As an example, Fig. 3 displays the wobble curve showing a system tuned to the ^{13}C and ^{23}Na nuclei at 11.7 Tesla (125.7 and 132.3 MHz, respectively). This scheme allows to benefit from the sensitivity gain of the *WIFI-NMRS* device for two different channels, and for instance in the present case to perform a ^{23}Na NMR image and a ^{13}C NMR spectrum without wiring change or further adjustment.

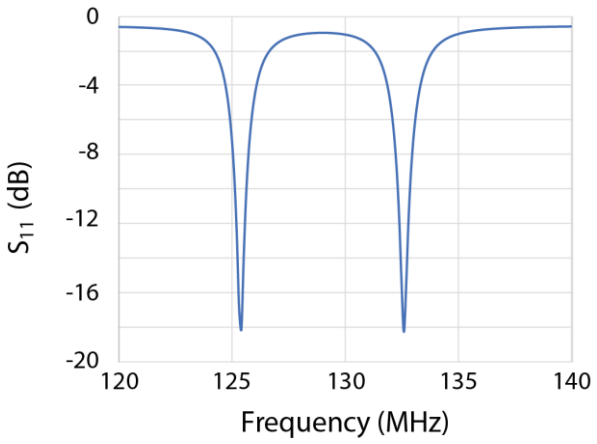

Figure 3. Example of signal reflected from the NMR probe (a 10-mm old generation BB probe) with an inductively-coupled insert aligned with a saddle coil. At 11.7 T, nuclei at two resonance frequencies can be studied with this setup: ^{13}C (125.7 MHz) and ^{23}Na (132.3 MHz). The NMR probe was originally tuned to 129 MHz – median value between the resonance frequencies - before introduction of the *WIFI-NMRS* insert.

For the purpose of testing not only the signal gain afforded by the NMR micro-detection system, but also the advantage presented by the controlled solution flow, in a second step NMR experiments have been performed with the *WIFI-NMRS* system installed on a micro-imaging probehead equipped with an 8-mm ^{13}C-^{1}H insert.

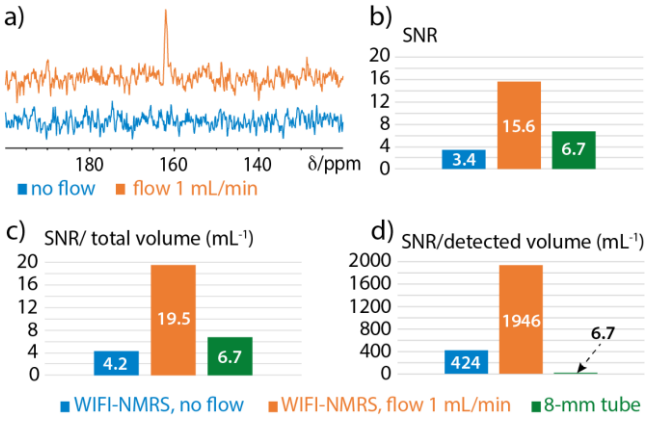

Figure 4. Data on the 10 mM ^{13}C-urea sample. a) ^{13}C NMR spectra acquired in 18 minutes with the WIFI-NMRS system with an interscan delay of 1s, on a static solution and with a gas flow of 1 mL/min. b) Comparison of the signal-to-noise ratios (SNR) obtained with the same experimental parameters for the WIFI-NMRS system (static and flow modes) and classical detection in an 8-mm NMR tube inside the commercial probehead. c) Idem, but SNR corrected by the total solution volume. d) SNR corrected by the detected volume. Other details: see the Supp. Info.

Figure 4 displays the ^{13}C NMR spectra obtained on a 10 mM ^{13}C-enriched urea sample in 1024 scans separated by a short delay of 1 s, without and with an air flow of 1 mL/min. The gain in signal-to-noise ratio between the flow and static modes is obvious in Fig. 4a, but Figs 4b-d enables one to compare the signal-to-noise ratios measured with the *WIFI-NMRS* device without and with solution flow, and with a classical (8-mm o.d.) NMR tube. In this purpose, the SNR values corrected by (divided by) the total solution volume are given in Fig. 4b. A gain by a factor 4.6 is observed in favor of the flowing solution over the static sample case. The SNR is also 1.9 higher than with the classical NMR tube. Note that for the present tests, an insert with an 800-µL solution circuit has been used, but this volume can be reduced to 300 µL in other versions (see Table S1). Considering the SNR corrected by the detection volume (Fig. 4d) further emphasizes the advantage of the approach. So, when it is reported to the detected volume, the gain between the on-flow mode of the *WIFI-NMRS* system and the classical detection in an 8-mm tube reaches now 289.2. Thus, due to the high sensitivity afforded by the micro-solenoid (shape efficiency and filling factor) and the solution flow in a closed loop, this setup compares favorably with the classical detection in NMR tubes, both in terms of mass- and concentration-based sensitivity.

In Supporting Information (Fig. S5) the signal-to-noise ratio has been reported as a function of the rf pulse flip angle, for two different interscan delays (0.5 and 1 s) and a gas flow of 1 mL/min. While for a recycling delay of 1 s the apparent Ernst angle is near 90°, it falls to *ca.* 75° for a recycling delay of 0.5 s. This means that despite a longer solution loop compared to our previous work, the gas flow is still able to efficiently pump the liquid with a decent flowrate. The fact that the apparent Ernst angle is ca. 90° with a recycling delay of 1 s means that all the solution in the detection region has been replaced in this time frame, allowing to fully circumvent relaxation. Since the detected volume in a 8 mm insert is 12.5 µL, we therefore can calculate the liquid flowrate which is 0.75 mL/min, for a gas flowrate of 1 mL/min. This value is coherent with our previous work, where the fluidic circuit was different but the principle was the same. [4]

This low-cost inductive device enables one to keep all the capabilities of the host probehead, such as the use of other rf channels. As an example, ^{13}C spectra have been recorded on a sample of ^{15}N-,^{13}C-enriched glycine in D_2O, with ^{1}H decoupling (Figure 5). Recording the spectra in the presence of a solution flow and an interscan delay of 1 s provides a SNR gain of 1.4 for the signal of the CH_2 group (1.3 when ^{1}H decoupling is applied), and of 3.4 for the signal of the CO group (2.9 when ^{1}H decoupling is applied). Note that the proton-carbon cross-relaxation comes to further enhance the signal and accelerate the apparent relaxation of ^{13}C, even (in a less extent) for the quaternary carbon. As expected on the spectrum of Fig. 5c the integral values of the two signals are identical within 1.3%.

Whereas these results have been obtained on 10- and 8-mm probes, which allowed us to assemble the *WIFI-NMRS* devices using quartz capillaries in the detection region (see figure S6), we are currently developing 5mm devices which would be of greater interest since most of the liquid-NMR probes are made for tubes of this diameter. Since the use of glass capillaries was compromised for these devices, due to the small length available (2 mm) for the capillary, we had to turn to another manufacturing technique. We chose to print the capillary along with the rest of the microfluidic device, therefore reducing the number of parts to be assembled. Using this technique, the printed parts already possess a complete fluidic circuit, while the coil still has to be wound around the capillary, which is made possible by designing an empty space around this printed capillary, which can later be filled with polymer, for susceptibility matching purposes.

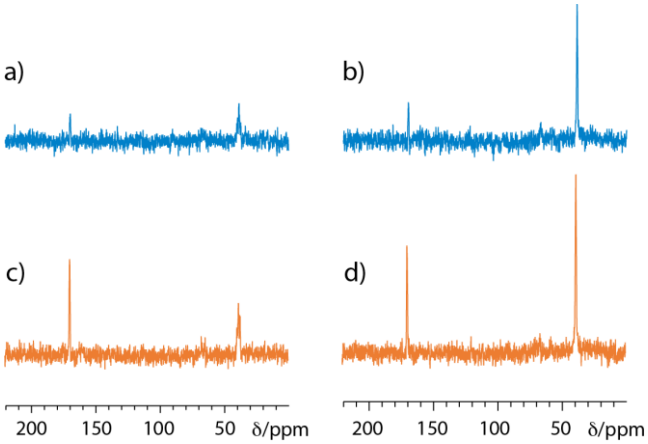

Figure 5. ^{13}C NMR spectra recorded in the same conditions with the *WIFI-NMRS* device on a 25-mM sample of ^{15}N-^{13}C-enriched glycine in D_2O, in static mode (a) and b)) and with a gas flow of 1 mL/min (c) and d)). In b) and d) ^{1}H decoupling was applied during acquisition. An interscan delay of 1s was used for all these acquisitions. Other details: see the Supp. Info.

To study the sensitivity of these 5 mm *WIFI-NMRS* devices, we used one of these tuned for ^{13}C with a sample of 200 mM ^{13}C Urea in D_2O. This device has been placed inside a 5 mm Bruker TBI probe. The results obtained with this configuration are presented in figure S7. The wobble curve easily shows that despite the small size of the solenoid and the large distance to the saddle coil (since we are using the outer coil of the inverse probe) we are able to get a good splitting indicating a strong coupling between the two coils. These preliminary results show that these smaller systems are prone to show the same advantages as the 10- and 8-mm ones discussed in this article.

Other on-flow solutions have been proposed to monitor in real time chemical systems without modifying the NMR instrument. For instance, Khajeh *et al.* developed an elegant and cheap solution involving a peristaltic pump outside the

NMR magnet.[18] However the *WIFI-NMRS* system presented here does not use large sample volumes: 300 – 800 µL in the presented versions, but that can further be reduced by decreasing the diameter of the 3D-printed channels. Another advantage of this system is that this volume is concentrated inside the highest magnetic field region of the magnet, ensuring a reliable pre-polarization.

In addition to be inexpensive – the only components are the 3D-printed inserts, the brass rod equipped with a Vernier, the tubing for the gas inlet, and the syringe pump - and adaptable on every high field NMR spectrometer, the *WIFI-NMRS* approach presents several advantages. i) The controlled solution flow enables avoiding the relaxation rate constraint, ii) the solenoidal micro-coil presents optimal shape and filling factor, iii) even with a single mono-tuned microcoil, it is possible to perform heteronuclear experiments, according to the host probe (^{1}H decoupling, X-^{1}H experiments), iv) the liquid flow can be used to transport hyperpolarized species to the NMR detection area and therefore increase the SNR.

Also, as the quality factor depends mostly of the host probe, the device will be very powerful when used in conjunction with cryoprobes.

ASSOCIATED CONTENT

Supporting Information

Video of the mini bubble pump in operation, wobble curve with the *WIFI-NMRS* insert, analysis of the magnetic flux from the solenoid insert through the probe, tuning of a Micro-5 probe using an additional capacitor, ^{23}Na MRI images performed with the *WIFI-NMRS* insert, detailed view of the 8-mm *WIFI-NMRS* insert, preliminary experiments with 5-mm inserts and experimental details. The Supporting Information is available free of charge on the ACS Publications website.

AUTHOR INFORMATION

Corresponding Author

* e-mail: patrick.berthault@cea.fr; Phone: +33 1 69084245.

ORCID

Guillaume Carret: 0000-0002-2083-3654
Patrick Berthault: 0000-0003-4008-2912

Notes

The authors declare no competing financial interests.

ACKNOWLEDGMENT

Support from the French Ministry of Research (project 17-LCV2-0002-01 LabCom DESIR) is acknowledged.

REFERENCES

(1) Laude, D. A.; Lee, R. W.; Wilkins, C. L. Analytical Applications of a Recycled Flow Nuclear Magnetic Resonance System: Signal Enhancement of Slowly Relaxing Nuclei. *Anal. Chem.* **1985**, *57* (7), 1281–1286.

(2) Fischer, H. H.; Seiler, M.; Ertl, T. S.; Eberhardinger, U.; Bertagnolli, H.; Schmitt-Willich, H.; Albert, K. Quantification Studies in Continuous-Flow 13C Nuclear Magnetic Resonance Spectroscopy by Use of Immobilized Paramagnetic Relaxation Agents. *J. Phys. Chem. B* **2003**, *107* (20), 4879–4886.

(3) Causier, A.; Carret, G.; Boutin, C.; Berthelot, T.; Berthault, P. 3D-Printed System Optimizing Dissolution of Hyperpolarized Gaseous Species for Micro-Sized NMR. *Lab. Chip* **2015**, *15* (9), 2049–2054.

(4) Carret, G.; Berthelot, T.; Berthault, P. Enhancing NMR of Nonrelaxing Species Using a Controlled Flow Motion and a Miniaturized Circuit. *Anal. Chem.* **2017**, *89* (5), 2995–3000.

(5) Doty, F. D. Probe Design and Construction. In *eMagRes*; John Wiley & Sons, Ltd, 2007.

(6) Hoult, D. I.; Richards, R. E. The Signal-to-Noise Ratio of the Nuclear Magnetic Resonance Experiment. *J. Magn. Reson.* **1976**, *24*, 71–85.

(7) Wei, X.; Wang, Z.; Dai, H. A Critical Review of Wireless Power Transfer via Strongly Coupled Magnetic Resonances. *Energies* **2014**, *7* (7), 4316–4341.

(8) Wang, T.; Ciobanu, L.; Zhang, X.; Webb, A. Inductively Coupled RF Coil Design for Simultaneous Microimaging of Multiple Samples. *Conc. Magn. Reson. B* **2008**, *33B* (4), 236–243.

(9) Ginefri, J.-C.; Rubin, A.; Tatoulian, M.; Woytasik, M.; Boumezbeur, F.; Djemai, B.; Poirier-Quinot, M.; Lethimonnier, F.; Darrasse, L.; Dufour-Gergam, E. Implanted, Inductively-Coupled Radiofrequency Coils Fabricated on Flexible Polymeric Material : Application to in Vivo Rat Brain MRI at 7T. *J. Magn. Reson.* **2012**, *224*, 61–70.

(10) Tang, J. A.; Jerschow, A. Practical Aspects of Liquid-State NMR with Inductively Coupled Solenoid Coils. *Magn. Reson. Chem.* **2010**, *48* (10), 763–770.

(11) Utz, M.; Monazami, R. Nuclear Magnetic Resonance in Microfluidic Environments Using Inductively Coupled Radiofrequency Resonators. *J. Magn. Reson.* **2009**, *198* (1), 132–136.

(12) Ludwig, U.; Eisenbeiss, A.-K.; Scheifele, C.; Nelson, K.; Bock, M.; Hennig, J.; von Elverfeldt, D.; Herdt, O.; Flügge, T.; Hövener, J.-B. Dental MRI Using Wireless Intraoral Coils. *Sci. Rep.* **2016**, *6*, 23301.

(13) Sakellariou, D.; Goff, G. L.; Jacquinot, J.-F. High-Resolution, High-Sensitivity NMR of Nanolitre Anisotropic Samples by Coil Spinning. *Nature* **2007**, *447* (7145), 694.

(14) Mispelter, J.; Lupu, M.; Briguet, A. *NMR Probeheads for Biophysical and Biomedical Experiments*; Imperial College Press, 2006; Vol. 1.

(15) Hoult, D. i.; Tomanek, B. Use of Mutually Inductive Coupling in Probe Design. *Conc. Magn. Reson.* **2002**, *15* (4), 262–285.

(16) Jacquinot, J.-F.; Sakellariou, D. NMR Signal Detection Using Inductive Coupling: Applications to Rotating Microcoils. *Conc. Magn. Reson. Part A* **2011**, *38A* (2), 33–51.

(17) Raad, A.; Darrasse, L. Optimization of NMR Receiver Bandwidth by Inductive Coupling. *Magn. Reson. Imag.* **1992**, *10* (1), 55–65.

(18) Khajeh, M.; Bernstein, M. A.; Morris, G. A. A Simple Flowcell for Reaction Monitoring by NMR. *Magn. Reson. Chem.* **2010**, *48* (7), 516–522.

Table of Contents artwork